

Figure 7.2.2. Blowing-up equation (7.2.10).

cones in the truncated symmetric systems are normally hyperbolic and hence persist under the addition of higher-order terms. We shall not consider this more complicated analysis here.

7.3. The Double Zero Eigenvalue

We now turn to a study of the degenerate 2- and 3-jets associated with the linear part $\begin{bmatrix} 0 & 1 \\ 0 & 0 \end{bmatrix}$, and a development of their universal unfoldings. As we

7.3. The Double Zero Eigenvalue

saw in the preceding section, the k -jet of

can be conveniently written in either of the forms

$$\dot{x} = y + \sum_{j=2}^k a_j x^j$$

$$\dot{y} = \sum_{j=2}^k b_j x^j$$

or

$$\dot{x} = y$$

$$\dot{y} = \sum_{j=2}^k (a_j x^j + b_j x^{j-1}) y$$

Takens [1974a] uses the first form while Bogdanov's [1975] uses the second. Here, in contrast to our treatment in Section 7.2, we shall follow Bogdanov's choice of the second form [1975] for another treatment.

We start with the assumption that the coefficients a_2, \dots, a_k and b_2, \dots, b_k do not vanish and initially neglect terms of order ϵ^0 . Then we drop the subscripts; thus we wish to unfold

$$\dot{x} = y,$$

$$\dot{y} = ax^2 + \dots$$

We shall see below that the signs of both a and b are important for the classification, and that both coefficients must be determined. (Applying the method of Bogdanov to the first form we find that we only require $a \neq 0$ and $b = 0$.)

A universal unfolding of (7.3.3) must contain all possible stable equilibria whose local flows contain all possible small loops. In contrast to the nice situation in the case of a double zero (Golubitsky and Schaeffer [1983]), here there is no simple formula for constructing such a family. Each case is different. In the present case, since the equilibrium at the origin is a center, it certainly be allowed to disappear or to split into two stable equilibria, but other nonwandering points may also be present in perturbations. The following figure shows a universal unfolding of (7.3.3):

$$\dot{x} = y,$$

$$\dot{y} = \mu_1 + \mu_2 y + \dots$$

We will sketch the justification of this assertion. The universal unfolding (7.3.4) differs from Bogdanov's [1975], because it contains more topological types in our unfolding as in his analysis.

saw in the preceding section, the k -jet of the normal form for this problem can be conveniently written in either of two ways:

$$\begin{aligned}\dot{x} &= y + \sum_{j=2}^k a_j x^j \\ &\quad + \mathcal{O}(|x, y|^{k+1}),\end{aligned}\tag{7.3.1}$$

or

$$\begin{aligned}\dot{x} &= y \\ &\quad + \mathcal{O}(|x, y|^{k+1}).\end{aligned}\tag{7.3.2}$$

$$\dot{y} = \sum_{j=2}^k (a_j x^j + b_j x^{j-1} y)$$

Takens [1974a] uses the first form while Bogdanov [1975] and Arnold [1972] take the second. Here, in contrast to our outlines of Takens' results in Section 7.2, we shall follow Bogdanov's choice. Also see Kopell and Howard [1975] for another treatment.

We start with the assumption that the quadratic coefficients a_2, b_2 do not vanish and initially neglect terms of order 3 and higher. As in Section 7.2, we drop the subscripts; thus we wish to unfold the degenerate vector field

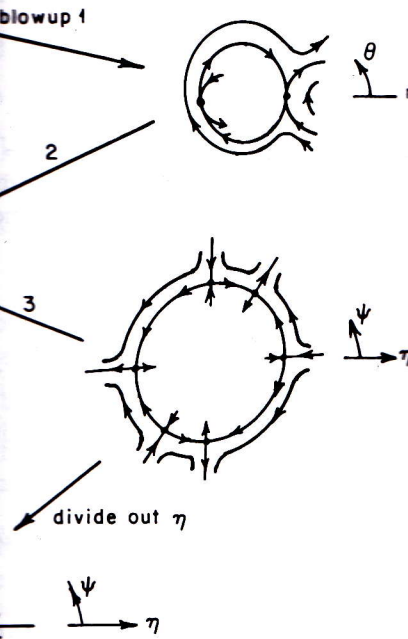
$$\begin{aligned}\dot{x} &= y, \\ \dot{y} &= ax^2 + bxy.\end{aligned}\tag{7.3.3}$$

We shall see below that the signs of both a and b are important in a topological classification, and that *both* coefficients must be nonzero for the unfolding to be fully determined. (Applying the methods of Section 7.2 to this normal form we find that we only require $a \neq 0$ for determinacy of the degenerate field.)

A universal unfolding of (7.3.3) must provide a family of vector fields whose local flows contain all possible small perturbations of the degenerate flow of (7.3.3). In contrast to the nice situation in singularity theory (cf. Golubitsky and Schaeffer [1983]), here there is no general recipe available for constructing such a family. Each case must be considered individually. In the present case, since the equilibrium point has a zero eigenvalue, it must certainly be allowed to disappear or to split into at least two structurally stable equilibria, but other nonwandering sets such as periodic orbits may also be present in perturbations. The following two-parameter family provides a universal unfolding of (7.3.3):

$$\begin{aligned}\dot{x} &= y, \\ \dot{y} &= \mu_1 + \mu_2 y + ax^2 + bxy.\end{aligned}\tag{7.3.4}$$

We will sketch the justification of this assertion later. We note that our form (7.3.4) differs from Bogdanov's [1975], but that we recover the same topological types in our unfolding as in his and in Takens' [1974b].



ing-up equation (7.2.10).

ystems are normally hyperbolic and hence
r-order terms. We shall not consider this

eigenvalue

generate 2- and 3-jets associated with the
ment of their universal unfoldings. As we

In our analysis, we fix a and b for simplicity. It should be clear that, with suitable rescaling and letting $(x, y) \rightarrow (-x, -y)$, for any $a, b \neq 0$ the possible cases can be reduced to two: $a = 1$ and $b = \pm 1$. We shall consequently take $a = b = 1$ and leave the other case as an exercise.

It is easy to find bifurcation curves in which (7.3.4) undergoes saddle-node and Hopf bifurcations. We first seek fixed points, which are given by

$$(x, y) = (\pm\sqrt{-\mu_1}, 0) \stackrel{\text{def}}{=} (x_{\pm}, 0), \quad (7.3.5)$$

and hence only exist for $\mu_1 \leq 0$. Linearizing at these points, we find

$$Df(x_{\pm}, 0) = \begin{bmatrix} 0 & 1 \\ \pm 2\sqrt{-\mu_1} & \mu_2 \pm \sqrt{-\mu_1} \end{bmatrix}. \quad (7.3.6)$$

Therefore $(x_+, 0)$ is a saddle for $\mu_1 < 0$ and all μ_2 , while $(x_-, 0)$ is a source for $\{\mu_2 > \sqrt{-\mu_1}, \mu_1 < 0\}$ and a sink for $\{\mu_2 < \sqrt{-\mu_1}, \mu_1 < 0\}$. Checking the conditions, we find that a Hopf bifurcation occurs on the curve $\mu_2 = \sqrt{-\mu_1}$ while saddle-node bifurcations occur on $\mu_1 = 0, \mu_2 \neq 0$.

EXERCISE 7.3.1. Verify the statements above.

To study the stability of the Hopf bifurcation, we change coordinates twice, first to bring the point $(x_-, 0)$ to the origin and then to put the vector field into standard form. Letting $\bar{x} = x - x_-, \bar{y} = y$, we obtain

$$\begin{pmatrix} \dot{\bar{x}} \\ \dot{\bar{y}} \end{pmatrix} = \begin{bmatrix} 0 & 1 \\ 2x_- & 0 \end{bmatrix} \begin{pmatrix} \bar{x} \\ \bar{y} \end{pmatrix} + \begin{pmatrix} 0 \\ \bar{x}\bar{y} + \bar{x}^2 \end{pmatrix}. \quad (7.3.7)$$

Then, using the linear transformation

$$\begin{pmatrix} \bar{x} \\ \bar{y} \end{pmatrix} = T \begin{pmatrix} u \\ v \end{pmatrix}, \quad (7.3.8)$$

where

$$T = \begin{bmatrix} 0 & 1 \\ \sqrt{-2x_-} & 0 \end{bmatrix}$$

is the matrix of real and imaginary parts of the eigenvectors of the eigenvalues $\lambda = \pm i\sqrt{-2x_-}$, we obtain the system with linear part in standard form:

$$\begin{pmatrix} \dot{u} \\ \dot{v} \end{pmatrix} = \begin{bmatrix} 0 & -\sqrt{-2x_-} \\ \sqrt{-2x_-} & 0 \end{bmatrix} \begin{pmatrix} u \\ v \end{pmatrix} + \begin{pmatrix} uv + \frac{1}{\sqrt{-2x_-}} v^2 \\ 0 \end{pmatrix}. \quad (7.3.9)$$

7.3. The Double Zero Eigenvalue

We can now use the stability algorithm. The non-vanishing terms are $f_{uv} = 1, f_{vv} = 2$. The coefficient in the normal form of the

$$a = \frac{1}{16\sqrt{-2x_-}} \cdot 1 \cdot \frac{2}{\sqrt{-2x_-}} =$$

The bifurcation is therefore *subcritical*. There are two periodic orbits surrounding the sink $(0, 0)$. We can summarize our knowledge so far: the (partial) bifurcation set and associated local dynamics. Check that the vector fields, and especially the nodes on $\mu_1 = 0$, are as shown in this diagram.

EXERCISE 7.3.2. Show that there are no periodic orbits for $\mu_1 > \sqrt{-\mu_2}, \mu_1 < 0$, and verify that the phase portrait is as sketched. In particular, use center manifold theory near the saddle and source-saddle connections sketched in Figure 7.3.1.

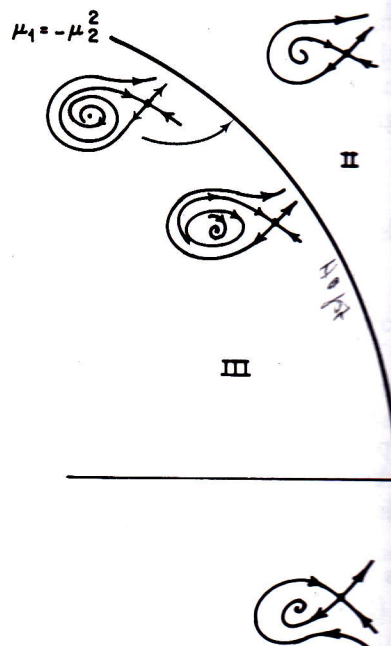


Figure 7.3.1. Unfolding equation (7.3.3), the double zero eigenvalue bifurcation. The diagram shows the phase plane with regions I, II, and III separated by the curve $\mu_2 = \sqrt{-\mu_1}$. The regions contain different types of equilibria: a source/sink at the origin in region I, a sink/source in region II, and a saddle in region III.

simplicity. It should be clear that, with $(-x, -y)$, for any $a, b \neq 0$ the possible $b = \pm 1$. We shall consequently take $b = \pm 1$. We shall consequently take $b = \pm 1$.

in which (7.3.4) undergoes saddle-node fixed points, which are given by

$$(-\mu_1, 0) \stackrel{\text{def}}{=} (x_{\pm}, 0), \quad (7.3.5)$$

arizing at these points, we find

$$\begin{bmatrix} 0 & 1 \\ -\mu_1 & \mu_2 \pm \sqrt{-\mu_1} \end{bmatrix}. \quad (7.3.6)$$

$\mu_2 < 0$ and all μ_2 , while $(x_{\pm}, 0)$ is a source for $\{\mu_2 < \sqrt{-\mu_1}, \mu_1 < 0\}$. Checking Hopf bifurcation occurs on the curve cations occur on $\mu_1 = 0, \mu_2 \neq 0$.

pf bifurcation, we change coordinates to the origin and then to put the vector $x - x_{-}, \bar{y} = y$, we obtain

$$\begin{pmatrix} \bar{x} \\ \bar{y} \end{pmatrix} + \begin{pmatrix} 0 \\ \bar{x}\bar{y} + \bar{x}^2 \end{pmatrix}. \quad (7.3.7)$$

$$T \begin{pmatrix} u \\ v \end{pmatrix}, \quad (7.3.8)$$

$$\begin{bmatrix} 0 & 1 \\ -2x_{-} & 0 \end{bmatrix}$$

ts of the eigenvectors of the eigenvalues with linear part in standard form:

$$\begin{pmatrix} u \\ v \end{pmatrix} + \begin{pmatrix} uv + \frac{1}{\sqrt{-2x_{-}}} v^2 \\ 0 \end{pmatrix}. \quad (7.3.9)$$

We can now use the stability algorithm (3.4.11). In this case, the only non-vanishing terms are $f_{uv} = 1, f_{vv} = 2/\sqrt{-2x_{-}}$ and we obtain the leading coefficient in the normal form of the Hopf bifurcation as

$$a = \frac{1}{16\sqrt{-2x_{-}}} \cdot 1 \cdot \frac{2}{\sqrt{-2x_{-}}} = \frac{1}{-16x_{-}} = \frac{1}{+16\sqrt{-\mu_1}} > 0. \quad (7.3.10)$$

The bifurcation is therefore *subcritical* and we have a family of *unstable* periodic orbits surrounding the sink for $\mu_2 < \sqrt{-\mu_1}$ and close to $\sqrt{-\mu_1}$. We can summarize our knowledge so far as in Figure 7.3.1, which shows the (partial) bifurcation set and associated phase portraits. The reader should check that the vector fields, and especially those of the degenerate saddle-nodes on $\mu_1 = 0$, are as shown in this figure.

EXERCISE 7.3.2. Show that there are no periodic orbits in the regions $\mu_1 > 0$ and $\mu_2 < -\sqrt{-\mu_1}, \mu_1 < 0$, and verify that the phase portraits of Figure 7.3.1 are correct. In particular, use center manifold theory near $\mu_1 = 0, \mu_2 \neq 0$ to show that the sink-saddle and source-saddle connections sketched above actually exist.

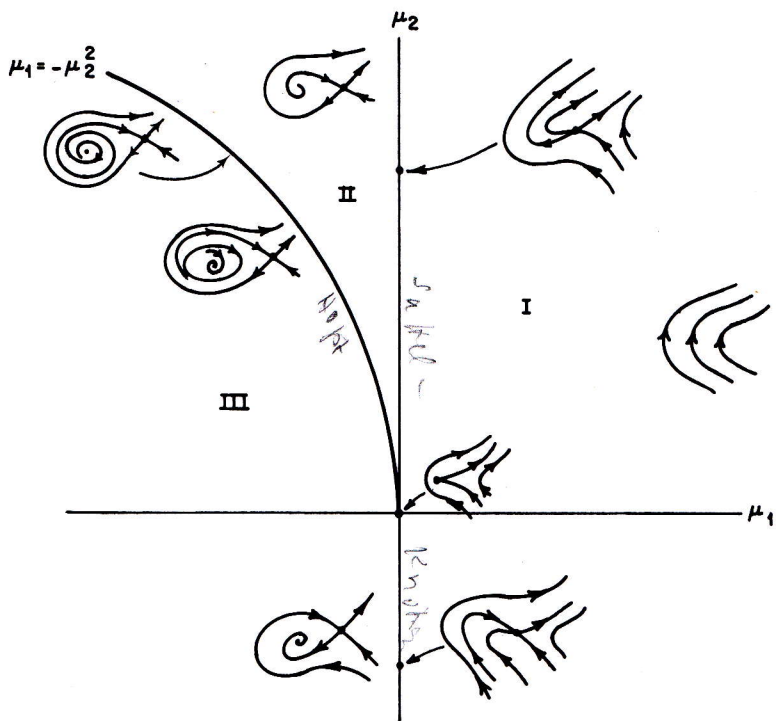


Figure 7.3.1. Unfolding equation (7.3.3), the partial bifurcation set and phase portraits of equation (7.3.4).

EXERCISE 7.3.3. Include the coefficient b in equation (7.3.4) explicitly in your calculations, and show that a *supercritical* Hopf bifurcation occurs if $b < 0$.

We now note that the phase portraits in region III near $\mu_1 = 0, \mu_2 < 0$ and $\mu_2 = \sqrt{-\mu_1} > 0$ are not homeomorphic, for the latter possess limit cycles while the former do not. Hence there must be additional bifurcation points in region III. The saddle and the sink do not change topological type in this region, and thus a *global* bifurcation must take place, perhaps a saddle loop (cf. Section 6.1) at which the limit cycle vanishes and the stable and unstable manifolds of the saddle point “cross over.” To study this, we use a rescaling transformation which differs somewhat from the blowing-up process described above (cf. Takens [1974b] and Carr [1981]). We set

$$x = \varepsilon^2 u, \quad y = \varepsilon^3 v, \quad \mu_1 = \varepsilon^4 v_1, \quad \mu_2 = \varepsilon^2 v_2, \quad \varepsilon \geq 0, \quad (7.3.11)$$

and rescale time $t \rightarrow \varepsilon t$, so that (with $a = b = 1$), (7.3.4) becomes

$$\begin{aligned} \dot{u} &= v, \\ \dot{v} &= v_1 + \varepsilon v_2 v + \varepsilon u v + u^2. \end{aligned} \quad (7.3.12)$$

The analysis of the unfolding now becomes the analysis of the *three*-parameter problem (7.3.12) with v_1, v_2 of $\mathcal{O}(1)$ and ε small. At first sight our transformation has merely introduced another parameter and enlarged the problem, but we note that we are only concerned with the case $v_1 < 0$ ($\mu_1 < 0$), since there are no fixed points for $v_1 > 0$; and, more significantly, if we let $\varepsilon \rightarrow 0$ with $v_1 \neq 0$ fixed, (7.3.12) becomes an integrable Hamiltonian system

$$\begin{aligned} \dot{u} &= v, \\ \dot{v} &= v_1 + u^2, \end{aligned} \quad (7.3.13)$$

with Hamiltonian

$$H(u, v) = \frac{v^2}{2} - v_1 u - \frac{u^3}{3}. \quad (7.3.14)$$

Using our singular transformation (7.3.11), we see that $\varepsilon = 0$ implies that $\mu_1 = \mu_2 = 0$, and our degenerate fixed point has blown-up into a Hamiltonian system. Moreover, the transformation keeps the fixed points a finite distance apart as the parameter approaches the degenerate bifurcation point $\mu_1 = \mu_2 = 0$.

The motivation for the rescaling is now apparent, since we can perturb the *global* solution curves of (7.3.13) for small ε , and hence reveal the behavior of (7.3.4) for μ_1, μ_2 close to zero. We might say that the Hamiltonian vector field of (7.3.13), with v_1 fixed (and we take $v_1 = -1$, corresponding to $\mu_1 \leq 0$) contains all the behavior of the unfolding “in embryo.” In particular, in Figure 7.3.2, note the closed orbits and the saddle connection Γ_0 corresponding to the level curve $H(u, v) = \frac{2}{3}$.

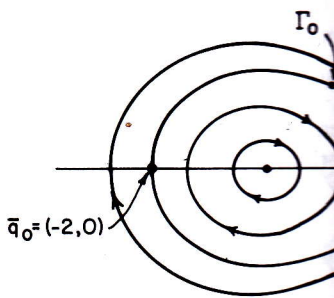


Figure 7.3.2. The phase portrait

The search for saddle loops is now reduced to finding the value of v_2 for which the saddle connection is maintained. The Melnikov function (Section 4.5–4.6) for the saddle connection at point $\bar{q}_0 = (-2, 0)$ is given by

$$(u_0(t), v_0(t)) = \left(1 - 3 \operatorname{sech}^2 \left(\frac{t}{\sqrt{2}} \right), 3 \right).$$

In this case the Melnikov function $M(v_2)$ is given by (7.3.14). The unperturbed situation is the constant vector field

$$\begin{aligned} M(v_2) &= \int_{-\infty}^{\infty} v_0(t)(v_2 v_0(t) - v_1) dt \\ &= \frac{1}{\sqrt{2}} \left[v_2 \int_{-\infty}^{\infty} 18 \operatorname{sech}^2 \left(\frac{t}{\sqrt{2}} \right) dt \right. \\ &\quad \left. + \int_{-\infty}^{\infty} (1 - 3 \operatorname{sech}^2 \left(\frac{t}{\sqrt{2}} \right))(-v_1) dt \right], \end{aligned}$$

where $\tau = t/\sqrt{2}$. The bifurcation situation, where the saddle connection is preserved, is given by $M \equiv 0$, or, for $v_2 = 0$,

$$v_2 \approx -\frac{\int_{-\infty}^{\infty} (1 - 3 \operatorname{sech}^2 \tau) d\tau}{\int_{-\infty}^{\infty} \operatorname{sech}^2 \tau d\tau}.$$

Noting that $\operatorname{sech}^2 \tau = 1 - \tanh^2 \tau$ and $\int_{-\infty}^{\infty} \operatorname{sech}^2 \tau d\tau = \pi$, we find that

$$\int_{-\infty}^{\infty} \operatorname{sech}^2 \tau \tanh^k \tau d\tau =$$

we find that

equation (7.3.4) explicitly in your calculations. This occurs if $b < 0$.

traits in region III near $\mu_1 = 0, \mu_2 < 0$ areomorphic, for the latter possess limit cycle there must be additional bifurcation the sink do not change topological type cation must take place, perhaps a saddle limit cycle vanishes and the stable and unstable "cross over." To study this, we use a different approach somewhat from the blowing-up [1974b] and Carr [1981]). We set

$$\dot{v}_1, \quad \mu_2 = \varepsilon^2 v_2, \quad \varepsilon \geq 0, \quad (7.3.11)$$

$a = b = 1$), (7.3.4) becomes

$$\dot{v}_2 v + \varepsilon u v + u^2. \quad (7.3.12)$$

comes the analysis of the three-parameter and ε small. At first sight our transformation parameter and enlarged the problem, but with the case $v_1 < 0$ ($\mu_1 < 0$), since there more significantly, if we let $\varepsilon \rightarrow 0$ with integrable Hamiltonian system

$$\dot{v}, \quad v_1 + u^2, \quad (7.3.13)$$

$$\frac{u^2}{2} - v_1 u - \frac{u^3}{3}. \quad (7.3.14)$$

(7.3.11), we see that $\varepsilon = 0$ implies that point has blown-up into a Hamiltonian which keeps the fixed points a finite distance from the degenerate bifurcation point $\mu_1 = 0$

is now apparent, since we can perturb for small ε , and hence reveal the behavior. We might say that the Hamiltonian and we take $v_1 = -1$, corresponding to the unfolding "in embryo." In particular, its and the saddle connection Γ_0 corresponds to $\varepsilon = \frac{2}{3}$.

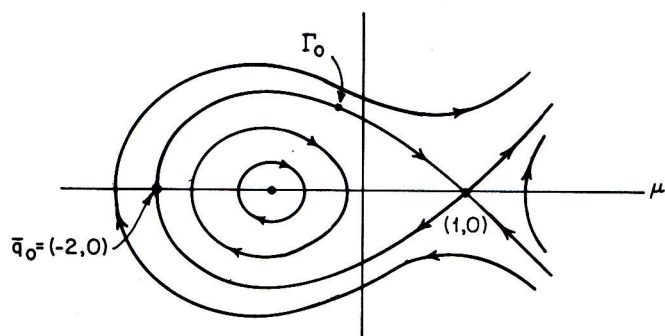


Figure 7.3.2. The phase portrait of (7.3.13), $v_1 = -1$.

The search for saddle loops is now a search for values of $v_2, \varepsilon \neq 0$ for which the saddle connection is maintained, a problem which we can solve by the Melnikov method (Sections 4.5–4.6). The solution on Γ_0 based at the point $\bar{q}_0 = (-2, 0)$ is given by

$$(u_0(t), v_0(t)) = \left(1 - 3 \operatorname{sech}^2 \left(\frac{t}{\sqrt{2}} \right), 3\sqrt{2} \operatorname{sech}^2 \left(\frac{t}{\sqrt{2}} \right) \tanh \left(\frac{t}{\sqrt{2}} \right) \right). \quad (7.3.15)$$

In this case the Melnikov function $M(t_0)$ is not time-dependent, since the perturbation is the constant vector field $\varepsilon \begin{pmatrix} 0 \\ v_2 v + uv \end{pmatrix}$, and we have

$$\begin{aligned} M(v_2) &= \int_{-\infty}^{\infty} v_0(t)(v_2 v_0(t) + u_0(t)v_0(t)) dt \\ &= \frac{1}{\sqrt{2}} \left[v_2 \int_{-\infty}^{\infty} 18 \operatorname{sech}^4 \tanh^2 \tau d\tau \right. \\ &\quad \left. + \int_{-\infty}^{\infty} (1 - 3 \operatorname{sech}^2 \tau) 18 \operatorname{sech}^4 \tau \tanh^2 \tau d\tau \right], \end{aligned} \quad (7.3.16)$$

where $\tau = t/\sqrt{2}$. The bifurcation situation, when the saddle connection is preserved, is given by $M \equiv 0$, or, for ε small:

$$v_2 \approx -\frac{\int_{-\infty}^{\infty} (1 - 3 \operatorname{sech}^2 \tau) \operatorname{sech}^4 \tau \tanh^2 \tau d\tau}{\int_{-\infty}^{\infty} \operatorname{sech}^4 \tau \tanh^2 \tau d\tau}.$$

Noting that $\operatorname{sech}^2 \tau = 1 - \tanh^2 \tau$ and that

$$\int_{-\infty}^{\infty} \operatorname{sech}^2 \tau \tanh^k \tau d\tau = \frac{\tanh^{k+1}(\tau)}{k+1} \Big|_{-\infty}^{\infty} = \frac{2}{k+1},$$

we find that

$$v_2 = \frac{5}{7}, \quad (7.3.17)$$

Finally, recalling that $v_1 = -1$ and using (7.3.11) ($\mu_1 = -\varepsilon^4$, $\mu_2 = \varepsilon^2 v_2$), we obtain the approximate bifurcation curve

$$\mu_1 = -\left(\frac{49}{25}\right)\mu_2^2, \mu_2 \geq 0. \quad (7.3.18)$$

The true bifurcation curve will be tangent to this semi-parabola at $\mu_1 = \mu_2 = 0$. Comparing this with the equation for the Hopf bifurcation set B_h :

$$\mu_1 = -\mu_2^2; \quad \mu_2 > 0, \quad (7.3.19)$$

we see that there is, indeed, a second bifurcation curve B_{sc} lying to the left of (7.3.19) and tangent to it (and to $\mu_1 = 0$) at $(\mu_1, \mu_2) = (0, 0)$. On B_{sc} the phase portrait has a saddle loop. The sign taken by the Melnikov function M for $\mu_1 >$ (resp. $<$) $-\left(\frac{49}{25}\right)\mu_2^2$ gives the relative position of the stable and unstable manifolds (separatrices of the saddle), and to conclude, we note that the trace of the "saddle quantity" (cf. Section 6.1) is positive on the curve (7.3.18):

$$\text{tr } Df(+\sqrt{-\mu_1}, 0) = \mu_2 + \sqrt{-\mu_1} = \frac{12}{5}\mu_2 > 0, \quad (7.3.20)$$

and thus that the homoclinic orbit is an α -limit set for nearby points. We illustrate this in Figure 7.3.3.

It remains to check that, throughout region IIIa, the system has a unique repelling limit cycle for each pair of parameter values (μ_1, μ_2) . Letting $\gamma = (u_\alpha(t), v_\alpha(t))$ denote one of the closed orbits within Γ_0 with Hamiltonian $H(u_\alpha, v_\alpha) = \alpha$ and period T_α , it is sufficient by Melnikov theory to verify that

$$\begin{aligned} M^\alpha(v_2) &= \int_0^{T_\alpha} v_\alpha(t)[v_2 v_\alpha(t) + u_\alpha(t)v_\alpha(t)] dt \\ &= \int_{\gamma^\alpha} [v_2 v + uv] du \end{aligned} \quad (7.3.21)$$

is zero for just one parameter value $v_2(\varepsilon, \alpha)$ for each choice of ε and α . This can be done either by direct evaluation of the integrals, using elliptic functions, or by arguments of the type used by Carr [1981]. We do not give the details here, but leave the computation as an exercise:

EXERCISE 7.3.4. Convert (7.3.16) into a contour integral around the homoclinic orbit and evaluate it. Evaluate (7.3.21) using elliptic functions (substitute $v = \sqrt{2\alpha + 2v_1 u + \frac{2}{3}u^2}$ from (7.3.14)). You might find Byrd and Friedman [1971] useful.

EXERCISE 7.3.5. Find the bifurcation set and phase portraits for the unfoldings of (7.3.4) with $a = +1, b = -1$; hence show that the choice $a = b = 1$ essentially captures all the cases up to reversal of time. What can you conclude when $b = 0$?

Note that the bifurcation set of Figure 7.3.3 is a set of codimension one curves meeting at the point, $\mu_1 = \mu_2 = 0$, at which the vector field has the codimension two singularity. On each curve a codimension one bifurcation takes place, saddle-nodes on $\mu_1 = 0; \mu_2 \neq 0$, Hopf on $\mu_1 = -\mu_2^2; \mu_2 > 0$

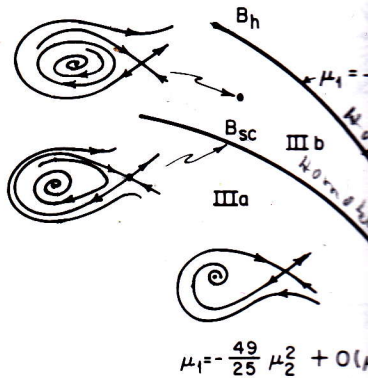


Figure 7.3.3. The global saddle connection.

and a saddle connection or homoclinic orbit for $\mu_2 > 0$. The latter is an example of a global bifurcation met before in Section 6.1. However, in the presence of such a global bifurcation, a local analysis will not suffice.

We will not address the problem of the global unfolding of (7.3.3) here. Indeed we have not discussed global unfoldings, for there are technical issues which prevent our treatment (cf. Newhouse et. al. [1978], Arnol'd [1972] and Bogdanov [1975] for examples).

EXERCISE 7.3.6. Show that the codimension one bifurcation point $(\sigma, \gamma) = (\frac{1}{2}, \frac{1}{2})$ in the averaged van der Pol equation (7.3.1) is a double zero eigenvalue point (cf. Holmes and Rand [1978]).

In the same [1974b] paper, Takens [1973] studied certain rotational symmetries. An important example of such a symmetry in the context of oscillations is that of "cubic" symmetry, $\pi/3$. Here the degenerate field contains a cubic term, and its global unfolding is provided by the two-parameter family

$$\dot{x} = y,$$

$$\dot{y} = \mu_1 x + \mu_2 y.$$

Allowing reversal and linear rescaling, we can assume without loss of generality, but there are two different possibilities, that

d using (7.3.11) ($\mu_1 = -\varepsilon^4$, $\mu_2 = \varepsilon^2 v_2$),
ion curve

$$\frac{49}{25}\mu_2^2, \mu_2 \geq 0. \quad (7.3.18)$$

gent to this semi-parabola at $\mu_1 = \mu_2 = 0$.
or the Hopf bifurcation set B_h :

$$\mu_2; \quad \mu_2 > 0, \quad (7.3.19)$$

bifurcation curve B_{sc} lying to the left of
 $\mu_1 = 0$) at $(\mu_1, \mu_2) = (0, 0)$. On B_{sc} the
sign taken by the Melnikov function M
the relative position of the stable and
the saddle), and to conclude, we note that
(cf. Section 6.1) is positive on the curve

$$\mu_2 + \sqrt{-\mu_1} = \frac{12}{5}\mu_2 > 0, \quad (7.3.20)$$

is an α -limit set for nearby points. We

out region IIIa, the system has a unique
of parameter values (μ_1, μ_2) . Letting
osid orbits within Γ_0 with Hamiltonian
ficient by Melnikov theory to verify that

$$[v_2 v_x(t) + u_\alpha(t) v_\alpha(t)] dt \\ + uv] du \quad (7.3.21)$$

$v_2(\varepsilon, \alpha)$ for each choice of ε and α . This
tion of the integrals, using elliptic func-
sed by Carr [1981]. We do not give the
on as an exercise:

a contour integral around the homoclinic
I) using elliptic functions (substitute $v =$
ight find Byrd and Friedman [1971] useful
and phase portraits for the unfoldings of (7.3.4)
the choice $a = b = 1$ essentially captures all
you conclude when $b = 0$?

Figure 7.3.3 is a set of codimension one
 $\mu_2 = 0$, at which the vector field has the
ch curve a codimension one bifurcation
 $\mu_1 = 0; \mu_2 \neq 0$, Hopf on $\mu_1 = -\mu_2^2; \mu_2 > 0$

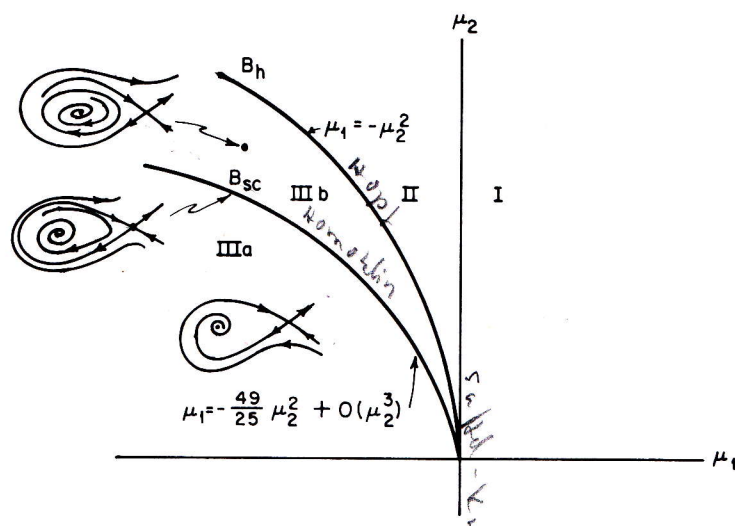


Figure 7.3.3. The global saddle connection bifurcation.

and a saddle connection or homoclinic bifurcation on $\mu_1 \approx -(\frac{49}{25})\mu_2^2; \mu_2 > 0$. The latter is an example of a global bifurcation which we have met before in Section 6.1. However, in this unfolding we have seen how the presence of such a *global* bifurcation can be detected by means of *local* analysis. This feature will occur repeatedly in this chapter.

We will not address the problem of proving that (7.3.4) is a universal unfolding of (7.3.3) here. Indeed we have not even clearly defined universal unfoldings, for there are technical issues at work here beyond the scope of our treatment (cf. Newhouse *et. al.* [1976]). Interested readers should consult Arnold [1972] and Bogdanov [1975] for more information on this particular example.

EXERCISE 7.3.6. Show that the codimension two bifurcation just described occurs at the point $(\sigma, \gamma) = (\frac{1}{2}, \frac{1}{2})$ in the averaged van der Pol equation (2.1.14) (cf. Section 2.1 and Holmes and Rand [1978]).

In the same [1974b] paper, Takens also studies unfoldings which preserve certain rotational symmetries. An important case in the study of nonlinear oscillations is that of “cubic” symmetry or symmetry under rotation through π . Here the degenerate field contains cubic terms at lowest order and the unfolding is provided by the two-parameter family

$$\begin{aligned} \dot{x} &= y, \\ \dot{y} &= \mu_1 x + \mu_2 y + a_3 x^3 + b_3 x^2 y. \end{aligned} \quad (7.3.22)$$

Allowing reversal and linear rescaling of time, we can set $b_3 = -1$ without loss of generality, but there are two distinct cases $a_3 = \pm 1$ to be considered.